Pathway to Diet- and Obesity-Associated Diabetes Through Attenuation of Pancreatic Beta Cell Glycosylation and Glucose Transport.

Kazuaki Ohtsubo, Mark Z. Chen, Jerrold M. Olefsky, Jamey D. Marth

Supplemental Figure 1

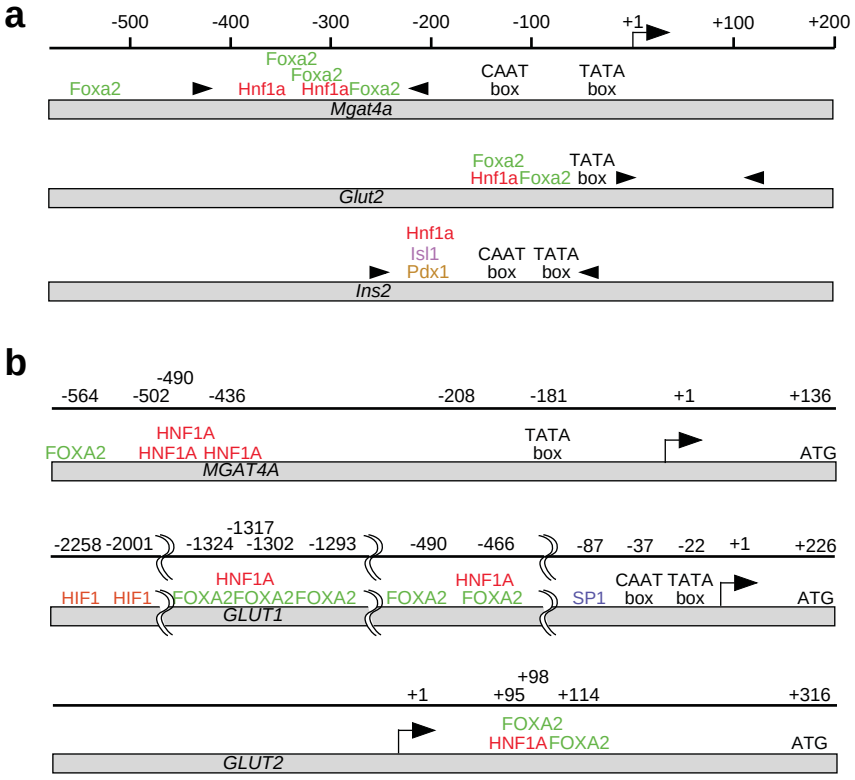

Fig. S1. Selected and mapped transcription factor binding motifs in the promoter regions of mouse *Mgat4a*, *Glut2*, and *Ins2* genes, and human *MGAT4A*, *GLUT1*, and *GLUT2* genes.
Transcription factor binding motifs for (**a**) mouse and (**b**) human genes were deduced by the TFBIND algorithm (Tsunoda and Takagi, 1999). The operational mouse *Glut2* promoter cis-elements are indicated as described (Cha et al., 2000). The operational mouse *Insulin2* promoter cis-elements are indicated as previously described (Mitanchez et al., 1997). The human *GLUT1* promoter structure was deduced by sequence alignment with rat *Glut1* promoter structure (Vinals et al., 1997; Santalucia et al., 1999) and the hypoxia inducible enhancer sequences (HIF-1 response element) were previously reported in the rat *GLUT1* promoter (Ebert et al., 1995; Chen et al., 2001). The operational human *GLUT2* promoter cis-elements are indicated as described (Cha et al., 2000; Holmquist et al., 2008).

Supplemental References

Cha, J-Y., Kim, H-i., Kim, K-S., Hur M-W., and Ahn, Y-H. Identification of transacting factor responsible for the tissue-specific expression of human glucose transporter type 2 isoform gene. *J.Biol.Chem.* **275**:18358-18365 (2000).

Chen, C., Pore, N., Behrooz, A., Ismail-Beigi, F., and Maity, A. Regulation of glut1 mRNA by hypoxia-inducible factor-1. *J. Biol. Chem.* **276**:9519-9525 (2001).

Ebert, B.L., Firth J.D., and Ratcliffe, P.J. Hypoxia and mitochondrial inhibitors regulate expression of glucose transporter-1 via distinct cis-acting sequences. *J.Biol.Chem.* **270**:29083-29089, (1995).

Holmkvist, J., Cervin, C., Lyssenko, V., Winckler, W., Anevski, D., Cilio,C., Almgren, P., Berglund, G., Nilsson, P., Tuomi, T., Lindgren, C.M., Altshuler, D. & Groop, L. Common variants in HNF-1 alpha and risk of type 2 diabetes. *Diabetologia* **49**, 2882-2891 (2006).

Mitanchez, D., Coiron, B., Chen, R., and Kahn, A. Glucose-stimulated genes and prospects of gene therapy for type I diabetes. Endocrine Reviews, 18:520-540 (1997).

Santalucia, T., Boheler, K.R., Brand, N.J., Sahye, U., Fandos, C., Vinals, F., Ferre, J., Testar, X., Palacin, M., and Zorzano, A. Factors involved in GLUT-1 glucose transporter gene transcription in cardiac muscle. *J. Biol. Chem.* **274**:17626-17634 (1999).

Tsunoda, T. & Takagi, T. Estimating transcription factor bindability on DNA. *Bioinformatics* **15**, 622-630 (1999).

Vinals, F., Fandos, C., Santalucia, T., Ferre, J., Testar, X., Palacin, M., and Zorzano, A. Myogenesis and MyoD down-regulate Sp1. *J. Biol. Chem.* **272**:12913-12921 (1997).

Supplemental Figure 2

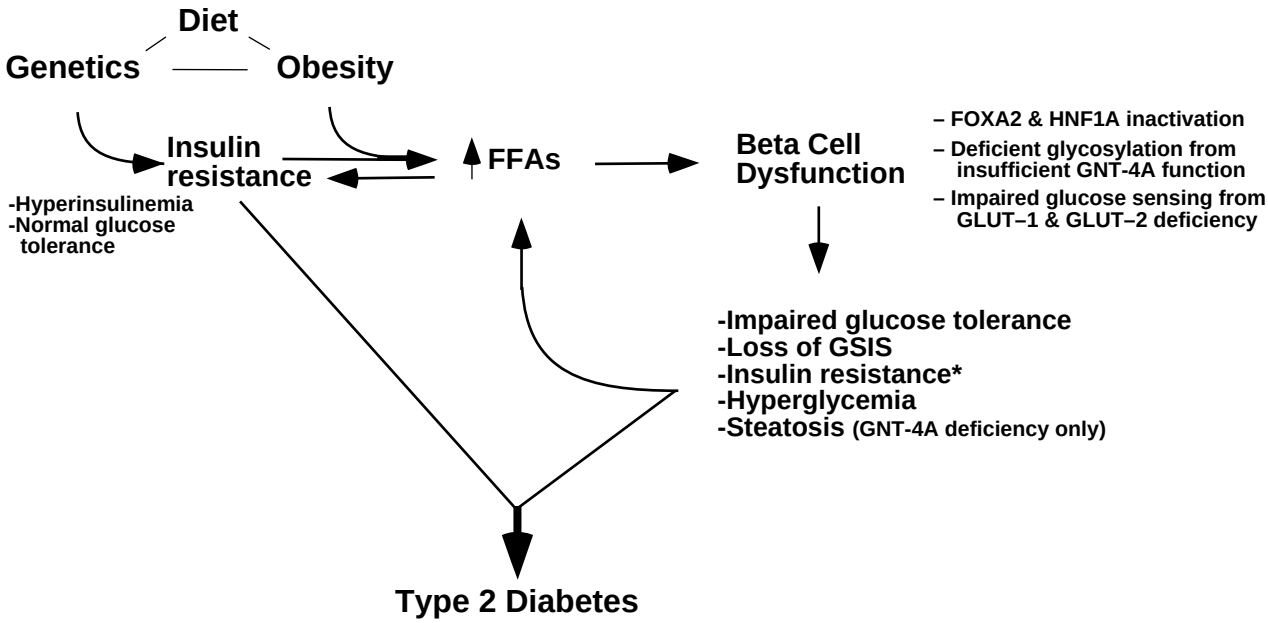

Fig. S2. Modeling pancreatic beta cell involvement in the pathogenesis of diet- and obesity-associated Type 2 diabetes. Genetics, diet, and obesity participate in a pathogenic pathway that encompasses beta cell dysfunction in the diagnosis of Type 2 diabetes. The genetics of individual inheritance may contribute to a pre-disease state that includes hyperinsulinemia and normal glucose tolerance in the presence of primary insulin resistance. Diet and obesity contribute to elevated free fatty acids (FFAs) in the blood, which can disrupt the expression and function of FOXA2 and HNF1A transctiption factors in beta cells. This impairs *MGAT4A* gene expression. The resulting defect in GNT-4A activity combines with reductions of *SLCA1* and *SLCA2* RNA expression to greatly reduce GLUT–1 and GLUT–2 glycoprotein residency and function at the beta cell surface. This results in diminished glucose uptake with loss of GSIS, impaired glucose tolerance, and insulin resistance. Beta cell dysfunction further contributes to systemic insulin resistance*, which can increase FFA levels in amplifying this pathologic cycle. Preservation of GNT-4A activity is uniquely capable of maintaining normal GLUT expression, glucose transport, and blocking the onset of steatosis.

Supplemental Figure 3

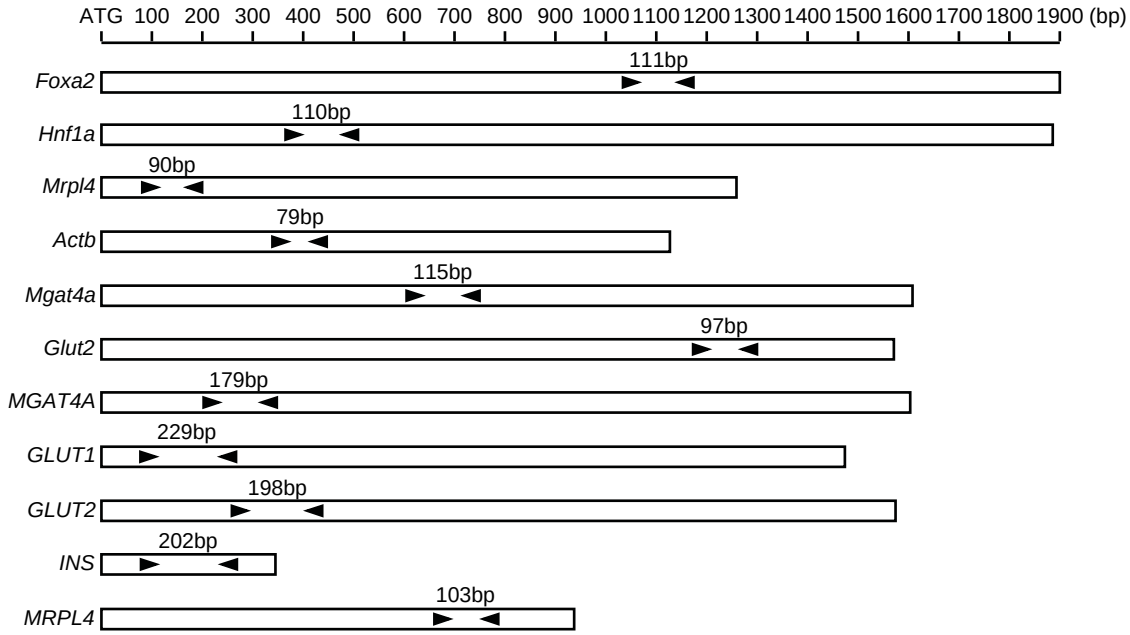

Fig. S3. Primer positions for detection and measurement of RNA transcript abundance using real-time PCR. Coding regions of indicated gene transcripts are represented as horizontally-extended open boxes. Primer positions are overlayed on a base-pair count from the initiating methione (ATG) codon and approximated as arrowheads. The bp sizes of amplified DNA fragments are also indicated.

Fig. S4. Transcription factor and cis-regulatory DNA sequence elements, and primer positions for ChIP analyses. Promoter and cis-regulatory sequences including transcription factor binding consensus elements, transcription start (+1) sites, and initating codons (Met) of human and mouse genes (**a**) *MGAT4A,* (**b**) *Mgat4a,* (**c**) *GLUT2*, (**d**) *Glut2*, (**e**) *INS*, (**f**) *Ins2*, (**g**) *GLUT1.* Primers (red) are designed to amplify indicated DNA fragments.

Nature Medicine doi:10.1038/nm.2414

Supplemental Table 1. Blood Chemistry

	C57BL/6J	RIP2-*MGAT4A*	RIP2-*GLUT2*
[Standard diet]	(n=25)	(n=25)	(n=25)
Glucose (fed) (mg/dl)	139.8±3.3	126.5±4.1	128.7±4.7
Glucose (fasting) (mg/dl)	98.12±4.4	107.2±2.8	106.1±4.2
Insulin (fed) (ng/ml)	0.65±0.06	1.05±0.08**	1.07±0.12
Insulin (fasting) (ng/ml)	0.13±0.02	0.15±0.01	0.15±0.01
Free fatty acid (fed) (mmol/l)	0.62±0.04	0.66±0.04	0.64±0.06
Free fatty acid (fasting) (mmol/l)	1.24±0.12	1.30±0.07	1.18±0.13
Triglyceride (mg/dl)	43.22±2.50	31.56±1.79***	29.48±2.27***
AST (IU/L)	66.15±5.67	75.93±5.16	85.16±8.98
ALT (IU/L)	35.96±2.42	35.27±2.95	40.84±4.90
Lipase (U/L)	54.28±5.36	49.20±1.96	45.61±1.66
Cholesterol (mg/dl)	57.93±2.23	62.96±2.95	53.10±1.32
HDL-cholesterol (mg/dl)	43.50±2.52	51.46±2.42**	47.73±3.22
[High-fat diet]	(n=16)	(n=16)	(n=16)
Glucose (fed) (mg/dl)	255.9±6.4	160.0±5.7***	182.8±8.5**
Glucose (fasting) (mg/dl)	231.3±7.6	142.6±8.6***	177.1±16.9**
Insulin (fed) (ng/ml)	5.95±0.63	3.21±0.57**	3.13±0.81**
Insulin (fasting) (ng/ml)	5.13±0.20	1.89±0.17***	2.10±0.24***
Free fatty acid (fed) (mmol/l)	1.14±0.14	0.84±0.07**	1.13±0.08
Free fatty acid (fasting) (mmol/l)	1.49±0.14	1.26±0.06	1.32±0.07
Triglyceride (mg/dl)	100.60±11.52	73.65±4.83*	75.17±7.70*
AST (IU/L)	102.10±13.66	94.78±8.57	116.2±12.97
ALT (IU/L)	63.39±11.47	70.11±8.38	81.67±11.26
Lipase (U/L)	51.89±1.75	50.44±1.71	49.33±3.04
Cholesterol (mg/dl)	141.60±6.94	138.4±5.53	139.2±11.44
HDL-cholesterol (mg/dl)	138.90±3.37	120.8±8.05	122.7±9.64

The asterisks indicate a significant difference between C57BL/6J and transgenic mouse line; *, $p<0.05$;**, $p<0.005$; ***, $p<0.001$ (Bonferroni test after ANOVA).

Supplemental Methods

Histology. For preparation of mouse tissue sections, anesthetized mice were pre-perfused with PBS at 1 ml min^{-1} flow rate through left ventricle for 15 min. Subsequently, the fixative (4% paraformaldehyde/PBS) was applied to the perfusion line for 15 min. After the continuous perfusion, organs were harvested and further fixed with the fixative for 3 hours. Following the post-fixation, the fixative was replaced to 20% sucrose/PBS and incubate at 4 °C for 16 hrs. The tissues were embedded in O.C.T. compound (Tissue-Tek). For immunofluorescence analyses, 5 μm tissue sections were incubated with antibodies to one or more molecules including GLUT–2 (AB1342, Chemicon Inc.), insulin (4011-01F, Linco Inc.), FOXA2 (07-633, Upstate biotechnology; M-20, Santa Cruz Biotechnology), HNF1A (ab96777, Abcam). The cell nucleus was counter-stained with DAPI (Molecular probe) or propidium iodide (PI, Sigma). Confocal microscopy including cell boundary assignment was accomplished by the automated TissueGnostics image analysis system (Vienna, Austria). Fluorescence was also quantified in some studies using MetaMorph software (Universal Imaging Corporation, Downington, PA).

siRNA transfection. siRNA targeting was performed by transfection of islet cells with the Stealth Negative control RNAi oligo (medium GC duplex, Invitrogen), the mouse Foxa2 Stealth select RNAi oligo duplex (UGCAUGACCUGUUCGUAGGCCUUGA, Invitrogen), the mouse HNF-1α Stealth RNAi oligo duplex (UAUAGGUGUCCAUGGCCAACUUGUG, Invitrogen), the human *GLUT1* Stealth RNAi oligo duplex (Invitorogen), and the human *GLUT2* Stealth RNAi Oligo duplex (Invitrogen) using Lipofectamine RNAiMAX reagent (Invitrogen) according to the manufacture instructions. After 72 hrs of culture with siRNAs, total cell RNA was

prepared and subjected to real-time PCR analyses. Gene expression levels were normalized to the expression of mouse or human mitochondrial ribosomal protein L4 (MRPL4).

mRNA preparation and quantitation by real-time PCR. Total RNA was prepared from samples using RNeasy Mini Kit (Qiagen), and then treated with DNase I (Invitrogen) to remove contaminated genomic DNA. Total RNA (1 μg) was subjected to reverse transcription using SuperScript III first-strand synthesis system (Invitrogen). Quantitative real-time PCR was performed using Brilliant SYBR Green Reagents (Stratagene) on Mx3000P QPCR System (Stratagene). Primers for real-time PCR were as follows: mouse Foxa2-RT-F (5'-AGCACCATTACGCCTTCAAC-3'); mouse Foxa2-RT-R (5'-CCTTGAGGTCCATTTTGTGG-3'); mouse HNF-1α-RT-F (5'-ACTTGCAGCAGCACAACATC-3'); mouse HNF-1α-RT-R (5'-CTTCTGTGTCTTCATGGGTGTG-3'); mouse Glut2-RT-F (5'-ATTCGCCTGGATGAGTTACG-3'); mouse Glut2-RT-R (5'-CAGCAACCATGAACCAAGG-3'); mouse Mgat4a-RT-F (5'-CTGGCCTGCTGGAAATAATC-3'); mouse Mgat4a-RT-R (5'-CAGGTTTTGCTTGGTTCTCC-3'); mouse MRPL4-RT-F (5'-GTTCAAAGCTCCCATTCGAC-3'); mouse MRPL4-RT-R (5'-AATTCACTGACGGCATAGGG-3'); mouse β-ACTIN-RT-F (5'-GGCCAACCGTGAAAAGATGA-3'); mouse β-ACTIN-RT-R (5'-CACAGCCTGGATGGCTACGT-3').); human MGAT4A-RT-F (5'-AACAGTTCAAGCGTGTAGGAGCAG-3'); human MGAT4A-RT-R (5'-TACAGCAGGTTGAAGACTTCCTTC-3'); human GLUT1-RT-F (5'-CTACAACACTGGAGTCATCAATGC-3'); human GLUT1-RT-R (5'-GGCCAGCAGGTTCATCATCAGCAT-3'); human GLUT2-RT-F (5'-

CCTTGGGCTGAGGAAGAGACTGTG-3'); human GLUT2-RT-R (5'-TGAAAACCCCATCAAGAGAGCTCC-3'); human INSULIN-RT-F (5'-GAACCAACACCTGTGCGGCTCACA-3'); human INSULIN-RT-R (5'-TTCCACAATGCCACGCTTCTGCAG-3'); human MRPL4-RT-F (5'-GACTTAACACACGAGGAGATGC -3'); human MRPL4-RT-R(5'-GCATGCTGTGCACATTTAGG -3'). Amplified DNA sequences and fragment sizes are depicted (**Fig. S3**). The relative mRNA levels among mice were calculated by comparing with littermate wild type control mouse samples, after normalization to expression of either beta-actin or mitochondrial ribosomal protein L4 (MRPL4).

Chromatin immunoprecipitation. Pancreatic islets (>90% beta cells) were isolated from C57BL/6J mice receiving either the SD or HFD for 3-8 weeks and equal numbers were subjected to cross-linking with 1% formaldehyde and washed with ice-cold PBS. Cells were sequentially washed with buffer I (10 mM HEPES, 0.25% Triton X-100, 10 mM EDTA, 0.5 mM EGTA), and then buffer II (10 mM HEPES, 200 mM NaCl, 1 mM EDTA, 0.5 mM EGTA) and then resuspended with lysis buffer (50 mM Tris-HCl (pH 8.1), 1% SDS, 10 mM EDTA and 1x protease inhibitor cocktail (Roche Molecular Biochemicals, Inc)), prior to sonication 6 times for 10 sec, followed by centrifugation. Supernatants were collected and diluted in buffer (20 mM Tris-HCl (pH 8.1), 1% Triton X-100, 150 mM NaCl, 2 mM EDTA) followed by incubation with 2 μg sheared salmon sperm DNA, 20 ml of pre-immune serum and protein A-sepharose. Samples were then incubated with antibodies to either FOXA2 (M-20; Santa Cruz Biotechnology), or HNF1A (C-19, Santa Cruz Biotechnology), or acetylated Histone 4 (06-866, Upstate Biotechnology). Precipitates were first washed with TSE I (20 mM Tris-HCl (pH 8.1),

0.1% SDS, 1% Triton X-100, 150 mM NaCl, and 2 mM EDTA), TSE II (20 mM Tris-HCl (pH 8.1), 0.1% SDS, 1% Triton X-100, 500 mM NaCl, 2 mM EDTA), then with buffer III (10 mM Tris-HCl (pH 8.1), 1% NP-40, 1% deoxycholate, and 0.25 M LiCl), and then three times with TE and extracted with 1% SDS, and 0.1 M $NaHCO_3$. Cross-linking was reversed by incubation at 65°C for 6 hrs, and DNA fragments were purified with QIAquick (Qiagen). PCR primers used to determine the enrichment of indicated sequences by ChIP assay included: mouse Mgat4a-CHIP-F (5'-CATTGCTTGCTCTTATGCAGCGGA-3'); mouse Mgat4a-ChIP-R (5'-GGCTGGTTCTGTCTATGGAAAACA-3'); mouse Glut2-ChIP-F (5'-CACTCTGGCTGGTCAGCTATTCAT-3'); mouse Glut2-ChIP-R (5'-TAGATTCCCAACCTCCTCAAAACC-3'); mouse Insulin2-ChIP-F (5'-AGGGCCCCTTGTTAAGACTCTAA-3'); mouse Insulin2-ChIP-R (5'-ACTGGGTCCCCACTACCTTTAT-3').); human MGAT4A-CHIP-F (5'-ATATGTGAAAGAGGACACAGGACAG-3'); human MGAT4A-ChIP-R (5'-AAGATGAGAACTCTAATGATCACAC-3'); human GLUT1-ChIP-F (5'-GAGGCAGAGAACTGCTTGAATCCG -3'); human GLUT1-ChIP-R (5'-GAACCAGCTCAACTGTATACTGGC -3'); human GLUT2-ChIP-F (5'-CAATTACTGCCACATAACACATGCC-3'); human GLUT2-ChIP-R (5'-GTCCAAGTCTAATCTTCTCAGCGGC-3'); human INSULIN-ChIP-F (5'-TAATGTGGAAAGTGGCCCAGGTGAG-3'); human INSULIN-ChIP-R (5'-GGGCTGAGGCTGCAATTTCCGGACC-3'). Amplified DNA sequences are depicted (**Fig. S4**). Enrichment was measured by real-time PCR accomplished by an Mx3000P QPCR System (Stratagene) using Brilliant SYBR Green (Stratagene). PCR reactions typically used 1/50 of DNA samples extracted. The size of PCR products was confirmed by agarose gel. Fold-

enrichment ratios were calculated from experimental Ct values, which were normalized against Ct values from normal IgG negative controls, and then calculated as the input percentages.

Flow cytometry. Islet cell surface glucose transporter expression was measured using antibodies to Glut-1 (N-20, Santa Cruz Biotechnology) and Glut-2 (AB1342, Chemicon Inc.), and GnT–4a function was analyzed by DSA lectin binding.

Glucose transport assay. Glucose transport was measured using 2-[N-(7-nitrobenz-2-oxa-1,3-diazol-4-yl)amino]-2-deoxy-D-glucose (2-NBDG, Molecular Probes). Islet cells ($1x10^5$) were washed and pre-incubated with HEPES-buffered Krebs-Ringer bicarbonate solution (KRBH) (10 mM HEPES, pH 7.4, 129 mM NaCl, 4.7 mM KCl, 1.2 mM KH_2PO_4, 1.2 mM $MgSO_4$, 2 mM $CaCl_2$, 5 mM $NaHCO_3$, and 0.1% BSA), containing 2.8 mM glucose at 37°C for 30 min, and then were incubated with 200 μM of 2-NBDG in KRBH containing 10 mM glucose at 37° for 2 min. Glucose transport was stopped by addition of 2 mM cytochalasin B in KRBH and then cells were subjected to flow cytometry. 2-NBDG uptake was measured by cell fluorescence using flow cytometry.

Insulin signaling. Mice were fasted 16 hrs prior to being anesthetized and injected with PBS or insulin (5 mU/g body weight) through the inferior vena cava. Mice were euthanized 2 min later and tissues were quickly harvested and stored in liquid N_2. Tissues were homogenized in lysis buffer (25 mM Tris-HCl (pH 7.4), 150 mM NaCl, 1% Triton X-100, 1 mM EGTA, 1x proteinase inhibitor cocktail (Roche), 1 mM $Na_4P_2O_7$, 20 mM NaF, 1 mM Na_3VO_4) at 4°C. After centrifugation to clarify, lysates were subjected to immunoblot analyses using antibodies to Akt-1 (B–1, Santa Cruz Biotechnology), phospho-Akt-1 (Thr 308) (06–678, Upstate Biotechnology),

IRS–1 (C-20, Santa Cruz Biotechnology), and phospho-IRS–1 (Ser 307) (2381, Cell Signaling Technology).

Nature Medicine doi:10.1038/nm.2414